"This is the peer reviewed version of the following article: Pla-Pagà L, Guirro M, Gual-Grau A, et al. Proteomic Analysis of Heart and Kidney Tissues in Healthy and Metabolic Syndrome Rats after Hesperidin Supplementation. Molecular Nutrition & Food Research. 2020 May;64(10):e1901063.***, which has been published in final form at https://doi.org/10.1002/mnfr.201901063.***

This article may be used for non-commercial purposes in accordance with Wiley Terms and Conditions for Use of Self-Archived Versions."

Proteomic analysis of heart and kidney tissues in healthy and metabolic syndrome rats after hesperidin supplementation

Laura Pla-Pagà[1,2], Maria Guirro[3,4], Andreu Gual-Grau[3], Albert Gibert-Ramos[3], Elisabet Foguet-Romero[4], Úrsula Catalán[2,5], Jordi Mayneris-Perxachs[4]*, Nuria Canela[5], Rosa M. Valls[2,1]*, Lluís Arola[a,1,3], Rosa Solà[a,2,1,6], Anna Pedret[a,1,2].

[a]LLA, RS and AP contributed equally as senior authors.

[1]Eurecat, Centre Tecnològic de Catalunya, Unitat de Nutrició i Salut, Reus, Spain.

[2]Universitat Rovira i Virgili, Facultat de Medicina i Ciències de la Salut, Functional Nutrition, Oxidation and Cardiovascular Disease Group (NFOC-SALUT), Reus, Spain.

[3]Nutrigenomics Research Group, Biochemistry and Biotechnology Department, Universitat Rovira i Virgili, Tarragona, Spain.

[4]Centre for Omic Sciences, Joint Unit Universitat Rovira i Virgili – Eurecat, Centre Tecnològic de Catalunya, Unique Scientific and Technical Infrastructures, Reus, Spain.

[5]Institut d'Investigació Sanitària Pere Virgili, Reus, Spain.

[6]Hospital Universitari Sant Joan, Reus, Spain.

Keywords: proteomics, hesperidin, metabolic syndrome, rats, heart, kidney.

Corresponding authors:

*Rosa M. Valls Zamora, PhD. Universitat Rovira i Virgili, Facultat de Medicina i Ciències de la Salut, Functional Nutrition, Oxidation and Cardiovascular Disease Group. C/Sant Llorenç 21, 43201 Reus, Spain. Tel:(+34)977759375. E-mail:rosamaria.valls@urv.cat

*Jordi Mayneris-Perxachs. Centre for Omic Sciences, Joint Unit Universitat Rovira i Virgili – Eurecat, Centre Tecnològic de Catalunya, Unique Scientific and Technical Infrastructures. Av/ Universitat 1, 43204 Reus, Spain. Tel:(+34)977775539. E-mail:jmayneris@idibgi.org

Abbreviations

CAFH: cafeteria diet with hesperidin supplementation by vehicle

CAFV: cafeteria diet and vehicle (without hesperidin supplementation)

CVDs: cardiovascular diseases

CVRFs: cardiovascular risk factors

HED: human equivalent dose

HS: hesperidin supplementation

HOMA: hometostasis model assessment

IPA: ingenuity pathway analysis

MS: metabolic syndrome

OPLS-DA: orthogonal projection to latent structures discriminant analysis

PCA: principal component analysis

PLS-DA: partial least squares discriminant analysis

RIPA: radioimmunoprecipitation assay buffer

STDH: standard diet with hesperidin supplementation by vehicle

STDV: standard diet and vehicle (without hesperidin supplementation)

TMT: tandem mass tag

VIP: variable importance on projection

ABSTRACT

Scope

Proteomics has provided new strategies to elucidate the mechanistic action of hesperidin, a flavonoid present in citrus fruits. Thus, the aim of the present study was to determine the effects of hesperidin supplementation (HS) on the proteomic profiles of heart and kidney tissue samples from healthy and metabolic syndrome (MS) rats.

Methods and results

Twenty-four Sprague-Dawley rats were randomized into 4 groups: healthy rats fed a standard diet without HS, healthy rats administered HS (100 mg/kg/day), MS rats without HS, and MS rats administered HS (100 mg/kg/day) for 8 weeks. Heart and kidney samples were obtained, and proteomic analysis was performed by mass spectrometry. Multivariate, univariate and ingenuity pathways analyses were performed. Comparative and semiquantitative proteomic analyses of heart and kidney tissues revealed differential protein expression between MS rats with and without HS. The top diseases and functions implicated were related to the cardiovascular system, free radical scavenging, lipid metabolism, glucose metabolism and renal and urological diseases.

Conclusions

This study is the first to demonstrate the protective capacity of hesperidin to change to the proteomic profiles in relation to different cardiovascular risk biomarkers in the heart and kidney tissues of MS rats.

1. INTRODUCTION

Diets rich in fruits and vegetables are known to protect against cardiovascular diseases (CVDs), [1, 2] which include heart failure, stroke and chronic kidney diseases and are the leading cause of mortality worldwide.[3] Several studies have aimed to elucidate the beneficial role of bioactive compounds present in food, such as phenolic compounds, which have shown beneficial effects on different cardiovascular risk factors (CVRFs)[4] and on the prevention of CVDs,[5] to determine their mechanisms of action and identify biomarkers of disease or treatment response. In this sense, omics sciences have gained attention since they can provide important biological information on many biomolecules. Proteomics, one of the most common omics sciences involves large-scale protein identification to study the proteome of a tissue or organ under certain conditions. In cardiovascular research, proteomics can help to elucidate the signaling mechanisms involved in CVDs[6] and facilitate prevention and drug development.[7]

In recent years, citrus, particularly orange and orange juice, has been investigated in cardiovascular research. Citrus is rich in polyphenols, mainly flavonoids and lignans, with hesperidin (hesperetin-7-O-rutinoside) being the most abundant. Hesperidin has been assessed in studies on rats and humans and shown to have beneficial effects on several parameters related to the cardiovascular system and the improvement of CVRFs, such as decreasing blood pressure,[8–11] improving endothelium-dependent vasodilation during hypertension,[12] decreasing total cholesterol and triglyceride levels,[13] improving glucose and insulin levels and the HOMA index,[14] decreasing inflammatory markers,[9] decreasing kidney damage markers[15] and decreasing oxidative stress.[16]

However, proteomic analyses of the effects of citrus on health are scarce. Some studies analyzed the orange proteome but only for technological purposes[17, 18]. To the best of our knowledge, only one study performed an interventional analysis of orange juice consumption in humans to evaluate the proteomic changes in the peripheral blood mononuclear cells of healthy humans after consumption of a high-fat and high-carbohydrate meal to evaluate oxidative stress and inflammatory markers.[19] In this study, orange juice suppressed diet-induced inflammation. Furthermore, only one study evaluated the effects of hesperidin on the proteomic profile of human HepG2 cells in relation to cell death.[20] Therefore, no studies have examined the effects of hesperidin on the human or rat tissue proteome in relation to CVD or CVRFs despite several publications reporting a beneficial effect of hesperidin. Furthermore, the biological

processes by which hesperidin can induce cardioprotective effects have not been elucidated through proteomic analyses.

Therefore, the aim of this work was to determine the changes in the proteomic profiles of heart and kidney tissues in healthy and metabolic syndrome (MS) rats after hesperidin supplementation to shed light on the hesperidin mechanism of action.

2. EXPERIMENTAL SECTION

2.1. Animals and experimental design

The animal procedures were conducted in accordance with the guidelines of the EU Directive 2010/63/EU for animal experiments and approved by the Government of Catalonia and the Animal Ethics Committee of the University Rovira i Virgili (number 10061). Twenty-four eight-week-old male Sprague-Dawley rats (Charles River Laboratories, Wilmington, Massachusetts, USA) were randomly assigned to one of the following four groups (n=6 per group): healthy rats fed a standard diet and supplemented with milk as a vehicle (STDV), healthy rats fed a standard diet and supplemented with milk containing hesperidin (STDH), MS-rats fed a cafeteria diet supplemented with milk as a vehicle (CAFV) and MS-rats fed a cafeteria diet supplemented with milk containing hesperidin (CAFH); all of the treatments occurred over 8 weeks. The experimental design was the same as that described in Guirro M et al. 2018.[21]

2.2. Dosage information

Hesperidin was administered daily and orally via low-fat condensed milk over 8 weeks at a dose of 100 mg/kg of body weight/day. The rationale for choosing this dose was based on the beneficial effects of hesperidin reported in previous works focused on MS factors in rat models. [14, 22] Accordingly, the human equivalent dose (HED) of 100 mg/kg hesperidin was 1350 mg per day for a 60 kg human,[21, 23] a dose achievable with hesperidin-rich orange juice.

2.3. Kidney and heart proteomic analysis

Heart and kidney tissue samples were obtained immediately after the animals were sacrificed, snap-frozen in liquid nitrogen and stored at -80ºC until the analyses were performed.

Protein extraction and quantification

Sample tissue was weighed (25-30 mg) to perform cell lysis. According to the radioimmunoprecipitation assay buffer (RIPA) protocol (ThermoFisher Scientific, Barcelona, Spain). First, the samples were frozen in liquid nitrogen for complete lysis. The samples were then mixed with 1 mL of RIPA buffer, homogenized completely with a BlueBender via freeze thaw cycles, agitated for 1 h at 4ºC and centrifuged. After centrifugation, the samples were sonicated with a 30 s pulse at 50% amplitude. The samples were then centrifuged at 21,130 relative centrifugal force (RCF) for 15 minutes, and the supernatants were collected for protein precipitation with the addition of 10% trichloroacetic acid/acetone. The protein pellets were resuspended in 6 M urea/50 mM ammonium bicarbonate (ABC) and quantified by Bradford's method.

Protein digestion and peptide 10-plex tandem mass tag (TMT) labeling

Thirty micrograms of total protein was reduced with 4 mM 1.4-dithiothreitol (DTT) for 1 h at 37°C and alkylated with 8 mM iodoacetamide (IAA) for 30 minutes at 25ºC in the dark. Afterwards, the samples were digested overnight (pH 8, 37ºC) with sequencing-grade trypsin (Promega, Wisconsin, USA) at an enzyme:protein ratio of 1:50. Digestion was quenched by acidification with 1% (v/v) formic acid, and peptides were desalted on an Oasis HLB SPE column (Waters, California, USA) before TMT 10-plex labeling (Thermo Fisher, Scientific, Massachusetts, USA) according to the manufacturer's instructions.

For normalization of all samples in the study along with the different TMT-multiplexed batches, a pool containing all the samples was labeled with a TMT-126 tag and included in each TMT batch. The different TMT 10-plex batches were desalted on Oasis HLB SPE columns before nanoLC-MS analysis.

Off gel-nanoLC-(Orbitrap) MS/MS analysis

Labeled and multiplexed samples were fractionated by off-gel technology (Agilent, California, USA) according to the manufacturer's protocol. Samples were fractioned on 12 cm non-linear pH 3-10 strips in 12 fractions. Thus, fraction 1 (F1) was mixed with fraction 7 (F7), F2 was mixed with F8, and this protocol was repeated with all fractions. In total, 6 fractions were obtained, and they were separated on a C-18 reversed-phase (RP) nanocolumn (75 µm I.D; 15 cm length; 3 µm particle diameter, Nikkyo Technos Co, LTD, Japan) on an EASY-II nanoLC made by Thermo Fisher Scientific (Massachusetts, USA). The chromatographic separation was performed with a 90-minute gradient using Milli-Q water (0.10 % formic acid) and acetonitrile (0.10 % formic acid) as the mobile phase at a flow rate of 300 nL/min.

Mass spectrometry analyses were performed on an LTQ-Orbitrap Velos Pro made by Thermo Fisher via an enhanced FT-resolution MS spectrum (R=30000 FHMW) followed by a data-dependent FT-MS/MS acquisition (R=15000 FHMW, 40% HCD) of the 10 most intense parent ions with a charge state rejection of one and a dynamic exclusion of 0.5 minutes.

Protein identification and quantification

Protein identification and quantification were performed with Proteome Discoverer software v.1.4.0.288 (Thermo Fisher Scientific, Massachusetts, USA) using multidimensional protein identification technology (MudPIT), combining the 6 raw data files obtained after off-gel fractionation. For protein identification, all MS and MS/MS spectra were analyzed using the Mascot search engine (v.2.5). Mascot was set up to search SwissProt_2018_03.fasta database (557012 entries), restricted to *Rattus norvegicus* taxonomy (8003 sequences) and assuming trypsin digestion. Two missed cleavages were allowed, and errors of 0.02 Da for an FT-MS/MS fragmentation mass and 10 ppm for an FT-MS parent ion mass were allowed. TMT-10plex was set as the quantification modification, oxidation of methionine and acetylation of N-termini were set as dynamic modifications, and carbamidomethylation of cysteine was set as the static modification. For protein quantification, the ratios between each TMT-label and the 126-TMT label were used, and quantification results were normalized based on the protein median.

2.4. Statistical analysis

The proteins present in ≥67% of the samples in the 4 groups were considered for the statistical analysis. After the proteomic analysis, the data were log base 2 transformed, mean centered and Pareto scaled. The multivariate statistical analysis was performed using Metaboanalyst 4.0 (https://www.metaboanalyst.ca/). The modeling included the use of unsupervised methods such as principal component analysis (PCA), supervised methods such as partial least squares discriminant analysis (PLS-DA) and an orthogonal projection to latent structures discriminant analysis (OPLS-DA). For the univariate statistical analysis, the distribution of normality was assessed by Kolmogorov-Smirnov tests, and a t-test or a Wilcoxon test was performed for pairwise comparisons. The proteins that were statistically significant in univariate analysis with a p-value <0.01 and a PLS-DA variable importance on projection (VIP) score >1.5 in multivariate analysis were considered differentially expressed between groups.

2.5. Pathway analysis

The UniProt Database was used to obtain the gene symbols and protein description (https://www.uniprot.org/). Ingenuity pathway analysis (IPA; www.ingenuity.com) was used to analyze the protein networks via the statistically significant results from both multivariate and univariate analyses for biological interpretation. IPA was used to explores the possible metabolic cell signaling pathways that were over- or underrepresented by the experimentally determined proteins.

3. RESULTS

3.1. Biochemical analyses

In previous studies, [21, 24] the feeding of a cafeteria diet to Sprague-Dawley rats induced an obesogenic pattern with significant increases in body weight and fat mass, elevated systolic blood pressure, hypertriglyceridemia, hyperglycemia and high levels of low-density lipoprotein cholesterol (LDL-c), which are criteria required for MS diagnosis. Consequently, when applying the harmonized human definition of MS to Sprague-Dawley rats consuming a cafeteria diet, the rats exhibited a reflex of fat mass, elevated triglyceride (TG) levels (drug treatment for elevated TG is an alternate indicator), reduced high-density lipoprotein cholesterol (HDL-c) levels (drug treatment for reduced HDL-c is an alternate indicator), elevated blood pressure (systolic or diastolic (antihypertensive drug treatment in a person with a history of hypertension is an alternate indicator), and/or elevated fasting plasma glucose levels (drug treatment of elevated glucose is an alternate indicator).[25]

We also report that the consumption of hesperidin (100 mg/kg body weight/day) for 8 weeks improved lipid metabolism and the insulin response and decreased the systolic blood pressure in MS rats. In this sense, hesperidin supplementation can improve most of the MS criteria.[24]

3.2. Proteomic analysis results

From the proteomic analysis of heart and kidney tissue rat samples, 1127 and 1753 proteins were identified, respectively, and the total proteins identified from each tissue are detailed in **Supplementary Information Table 1** and **Supplementary Information Table 2**. The tables contain information on the protein IDs from UniProt, descriptions of the proteins, coverage, unique peptides identified, total peptides identified, peptide-to-spectrum matches, molecular weights, and the value for each protein.

3.2.1. Heart rat tissue proteomic analysis

For statistical analyses only those proteins that were present in ≥67% of the samples in the 4 groups were considered. After filtering, a total of 872 proteins were considered for statistical analysis. The identified proteins with a *p*-value <0.01 and a VIP score from PLS-DA>1.5 were considered significantly different between the STDV and STDH groups, and between the CAFV and CAFH groups.

Hesperidin effects in healthy rats fed a standard diet:

In multivariate analysis, no clear differences were observed between the 2 STD treatment groups (STDV versus STDH) in the unsupervised analysis. The supervised analysis showed that none of the assessed models were significant due to the negative performance measurement Q^2, indicating that the models were not predictive at all or were overfitted and that a random model would perform better. Moreover, the univariate analysis showed no significant differences between the treatment groups (STDV versus STDH) in any of the 872 considered proteins.

Hesperidin effects in MS rats fed a cafeteria diet:

In multivariate analysis, no clear differences between the 2 treatment groups (CAFV versus CAFH) were observed in CAF rats from the unsupervised analysis. The PLS-DA from the supervised analysis showed that a model including 1 component provided the best performance, as determined by the Q^2 measure. However, after permutation testing, the model was not found to be significant. Nevertheless, a borderline significant model with a strong predictive ability (Q^2Y=0.58, p=0.053) was obtained for the comparison between CAFH and CAFV rats. The univariate analysis showed 65 differentially expressed proteins between CAF groups with a *p*-value<0.01.

The proteins with a *p*-value<0.01 and a VIP score from PLS-DA>1.5 were considered to be differentially expressed between the group without hesperidin supplementation (CAFV) and the group with hesperidin supplementation (CAFH). A total of 35 proteins considered to be significantly different between the two groups met the 2 criteria of univariate and multivariate analyses. The information about the 35 proteins is detailed in **Table 1**. In total, 19 proteins were downregulated and 16 were upregulated after hesperidin treatment for 8 weeks compared to those in the CAFV group.

Pathway analysis of the heart tissue proteome:

IPA analysis was performed and the top signaling pathways that were significantly affected after hesperidin supplementation were obtained. The top 5 significant signaling pathways were: production of nitric oxide

and reactive oxygen species in macrophages (p=4.08E-04; ratio=0.021), which involved: APOA4, APOC2, CDC42 and RBP4; clathrin-mediated endocytosis signalling (p=4.50E-04; ratio=0,021), which involved: APOA4, APOC2, CLTC and RBP4; LXR/RXR activation (p=1.07E-03; ratio=0.028), atherosclerosis signaling (p=1.19E-03; ratio=0.027); and FXR/RXR activation (p=1.25E-03; ratio=0.026) which involved: APOA4, APOC2 and RBP4 in the last 3 canonical pathways.

Network of the heart tissue proteome:

The top networks found by IPA were "Molecular transport, carbohydrate metabolism and small molecule biochemistry" (score=16), "Cardiac arrhythmia, cardiovascular disease and metabolic disease" network (score=2) and "Cancer, cardiovascular disease and cell cycle" (score=2). The graphical representation of the top overlapping networks and the up- and downregulated proteins, symbolized in red or green, respectively, is shown in **Figure 1**. The proteins implicated in the top networks after hesperidin treatment for 8 weeks were: APOA4, SOD1, ATP5F1D, ATPA1A, SLC27A1, SLC25A3, OGDH, FLNA, ALDH7A1, CLTC and CDC42. The other proteins implicated in the top networks related to the proteins analyzed in the present study were: IL-1B, LAMC1, TNF, KCNJ11, ATP1B1, OTOF, SLC1A2, AP2B1, EPB41L2, GRM4, CACNA1B, F11R, TNFRSF1B, KCNJ2, CPT1A, PIN, MYO1C, PP2A, PRKCD, STAT3, NEFH, ITSN1, SRC, ABR, PRKCZ, CAMKII, FILIP1, AR, RCAN1, GSK3B, NFKB complex and SIPI.

3.2.2. Kidney rat tissue proteomic analysis

After filtering, a total of 1341 proteins were considered for the statistical analysis of kidney tissue samples. The identified proteins with a p-value<0.01 and a VIP score from PLS-DA>1.5 were considered significantly different between the STDV and STDH groups, and between the CAFV and CAFH groups.

Hesperidin effects in healthy rats fed a standard diet:

From the multivariate analysis no clear separation between the 2 STD groups (STDV versus STDH) was evident from the unsupervised or supervised analysis. From the univariate analysis, no statistically significant proteins were observed between the 2 STD groups among any of the 872 considered proteins.

Hesperidin effects in MS rats fed a cafeteria diet:

From unsupervised analysis, a clear separation between the 2 CAF groups (CAFV versus CAFH) was evident from the PCA, although it was not very clear in the hierarchical clustering analysis. A PLS-DA

from the supervised analysis showed that a model including 1 component provided the best performance, as determined by the Q^2 measurement. The OPLS-DA analysis showed a significant model with a strong predictive ability (Q^2Y=0.70, p=0.046) for the comparison between CAFH and CAFV rats. The univariate analysis showed 75 proteins that were differentially expressed between the 2 CAF groups with a p-value<0.01.

The proteins with a p-value<0.01 and a VIP score from PLS-DA>1.5 were considered to be differentially expressed between the groups with and without hesperidin supplementation. A total of 53 proteins were considered to be significantly different between the 2 groups met the 2 criteria from univariate and multivariate analyses. The information on the 53 proteins is detailed in **Table 2**. In total, 33 proteins were downregulated and 20 were upregulated after hesperidin treatment for 8 weeks compared to those in the CAFV group.

Pathway analysis of the kidney tissue proteome:

IPA analysis was performed and the top signaling pathways that were significantly affected in kidney tissue after hesperidin supplementation were obtained. The top 5 significant signaling pathways were: mitochondrial dysfunction (p=4.65E-06; ratio=0.039), which involved ATP5PF, COX6B1, CPT1A, OGDH, TXN2 and VDAC3; the sirtuin signalling pathway (p=9.37E-05; ratio=0.023), which involved: ATP5PF, CPT1A, HIST2H3C, SOD1, TIMM8B and VDAC3; xanthine and xanthosine salvage (p=2.82E-03; ratio=1), guanine and guanosine salvage I (p=5.62E-03; ratio = 0.5); and adenine and adenosine salvage I (p=5.62E-03; ratio=0.5), which involved PNP.

Network of the kidney tissue proteome:

The top network found by IPA was “Cellular compromise, free radical scavenging, cell death and survival” (score=14), followed by “Cell death and survival, free radical scavenging, organismal injury and abnormalities” (score=6) and “Cardiovascular system development and function, immunological disease, inflammatory disease” (score=1). The overlapping graphical representation of the 2 more important networks “Cellular compromise, free radical scavenging, cell death and survival” and “Cardiovascular system development and function, immunological disease, inflammatory disease”, as well as the and up- and downregulated proteins (in red and green, respectively) are represented in **Figure 2**. The proteins implicated in the top networks after hesperidin treatment for 8 weeks were EPB41L3, TXN2, SOD1, TPM3,

NUCB2, VDAC3, MYO1D, SLC25A3, OGDH, CPT1A, MME, CDC42, ABCG2 and RACK1. The other proteins implicated in the top networks related to the proteins analyzed in the present study were TNF, AGT, INSULIN, OTOF, SLC27A1, FRIN2B, TPM1, CD36, ITGB1, KCNJ11, CHMP2B, PLEC, KRT8, TPM2, MAPK14, HSPA5, PRKCZ, PAR6, NCF1, ERN1, EIF2AK3, CTSV and TP53.

3.3. Top diseases and functions determined from the heart and kidney tissue proteomes

Table 3 details the top relevant diseases and functions involving the significant proteins in both heart and kidney tissues. The top categories are the cardiovascular system, free radical scavenging, lipid metabolism, glucose metabolism and renal and urological diseases.

4. DISCUSSION

The current study presents the effects of hesperidin supplementation of 100 mg/kg body weight/day for 8 weeks on the proteomic profiles of heart and kidney tissues in rats with or without MS. Proteomic analysis revealed significant changes in the proteomic profiles of MS rats fed a cafeteria diet with and without hesperidin supplementation in both tissues after 8 weeks.

In the heart tissues of MS rats, 35 proteins were differentially expressed: 19 proteins were downregulated and 16 were upregulated. Moreover, in the kidney tissues of MS rats, 53 proteins were differentially expressed: 33 proteins were downregulated and 20 were upregulated.

Currently, there are no data on the effects of hesperidin polyphenol on the proteomes of heart and kidney tissues in healthy or MS rats. However, several studies have shown that polyphenols, such as resveratrol found in red wine and grapes and secoiridiods and hydroxytyrosol present in olive oil, can change the proteomes of cells, in rats and humans, improving different cardiovascular risk parameters such as inflammation, cholesterol homeostasis, oxidation and blood coagulation.[26–28]

Our results suggest that, in MS rats, hesperidin supplementation could exert cardioprotective effects by upregulating the expression of proteins related to the cardiovascular system such as ATP1A1 (1.32-fold). ATP1A1, found in heart tissue, is associated with ischemic acute renal failure when it is downregulated and with a decrease in blood pressure levels when it is up-regulated.[29] In addition, hesperidin can be cardioprotective by downregulating the expression levels of proteins known to affect blood pressure, such

as ATP5PF (-1.61-fold), which is found in kidney tissue and related to vasoconstriction, hypertension and cardiac hypertrophy in rats and humans.[30, 31] Another related protein that appeared to be downregulated in the kidney tissues of MS rats was TPT1 (-1.44-fold). TPT is implicated in the pathogenesis of atherosclerosis and pulmonary artery hypertension to prevent macrophage apoptosis in the artery intima.[32] IGFBP7 was also downregulated by hesperidin in kidney tissue (-1.69-fold). At high concentrations, this molecule is related to poor diastolic function and ventricular systolic pressure. Thus, elevated IGFBP7 levels could be a biomarker of diastolic dysfunction and functional capacity in humans with heart failure.[33]

Moreover, our findings suggest that hesperidin could also exert cardioprotective effects in MS rats by upregulating the expression levels of proteins related to free radical scavenging, such as ALDH7A1 (1.28-fold). ALDH7A1, found in heart tissue, protects cells against oxidative stress by metabolizing lipid peroxidation-derived aldehydes produced during oxidative stress and xenobiotics metabolism.[34] During lipid peroxidation, large quantities of aldehydes are produced, and they can covalently bind to proteins and DNA, inactivating different proteins and damaging DNA. However, aldehydes are related to several diseases, such as atherosclerosis.[35] In the heart and kidney tissues of MS rats, another protein upregulated by hesperidin was FLNA, a large cytoplasmic protein (1.54-fold in heart tissue and 1.20-fold in kidney tissue). FLNA can promote or suppress cell processes important for heart development.[36] FLNA is downregulated in rats with coronary microembolization,[37] and the lack of FLNA demonstrates its importance during morphogenesis of several organs, such as the heart; the lack of FLNA can result in cardiovascular malformations.[38] Moreover, the lack of editing in FLNA increased RhoA/Rock and PLC/PKC signaling, increased aortic hypercontraction and induced cardiomyocyte hypertrophy, increasing the diastolic blood pressure.[39]

Our results suggested that hesperidin downregulated CD2AP inducing changes in the expression of proteins related to glucose metabolism. CD2AP, a cytosolic protein that interacts with signaling molecules,[40] was downregulated in the kidney tissues (-1.27-fold) of MS rats. Evidence suggests that high levels of CD2AP increase the risk of renal disease in patients with diabetes.[41] Another differentially expressed and upregulated protein in kidney tissue was EPHX2 (4.26-fold). Decreased EPHX2 expression is related to

increased insulin sensitivity in humans with MS.[42] Accordingly, hesperidin supplementation could exert preventive effects on glucose metabolism in MS rats, but the effects of hesperidin intake on humans with CVRFs such as diabetes and MS need to be confirmed.

Although the present study showed that hesperidin supplementation can change the proteomic profile to exert positive effects on different parameters in MS rats, some differentially expressed proteins showed negative effects. For example, in MS rats, the following 2 antioxidant proteins were downregulated: SOD1 (-1.39-fold in heart tissue; -1.58-fold in kidney tissue) and TXN2 (-1.36-fold in kidney tissue), which likely decreased the protection against oxidative stress in MS rats. In addition, SLC9A3R1 was downregulated in kidney tissue (-1.25-fold). Decreased expression of SLC9A3R1 was found in hypertensive rats,[43] indicating that hesperidin supplementation does not exert a beneficial effect on it, at least not by this pathway. However, in MS rats, some proteins related to lipid metabolism were downregulated in the heart, such as APOA4 (-1.50-fold) and APOC2 (-1.83-fold). APOA4 increases triglyceride production and reduces hepatic lipids;[44] therefore, a decrease in its expression would be expected to interfere with the correct absorption and elimination of dietary fats. However, actual evidence has demonstrated that decreased levels of APOA4 increase the chylomicron size, delaying its clearance from the blood and indicating it is not required for triglyceride absorption in the mouse intestine.[45] Thus, more studies of hesperidin supplementation are needed to clarify these effects on the proteomic profile.

Additionally, in MS rats after administered hesperidin supplementation, some of the proteins differentially expressed in the heart and kidney tissues were related to cancer. In the heart tissues of MS rats, CCDC58 and SLC25A3 were upregulated (1.73-fold and 1.36-fold, respectively). CCDC58 is a biomarker of breast, endometrial and urethral cancer, and SLC25A3 is overexpressed in cervical carcinomas.[46] In the kidney tissues of MS rats, the proteins UQCRH and LZTFL1 were downregulated (-1.40-fold and -1.58-fold, respectively). In the literature, UQCRH overexpression is associated with a poor prognosis for lung cancer and hepatocellular carcinoma patients.[47, 48] Finally, LZTFL1 is a tumor suppressor and an independent prognostic marker for the survival of gastric cancer patients when it is elevated.[49] In this sense, several studies in cancer models have shown that hesperidin can delay cell proliferation,[50] inhibit cell viability

and induce apoptosis in cancer cells.[51] Therefore, studies of hesperidin supplementation in rats with cancer and its effects on the proteome are needed to provide more robust evidence and to clarify whether hesperidin could be a tumor suppressor.

The present study has several limitations that warrant discussion. One limitation is the small sample size. Based on the results obtained in the present work, further studies with larger sample sizes and other experimental models, such as diabetes and cancer, will be performed to confirm the observed effects. Additionally, the dose of hesperidin should be increased or decreased to observe the different effects of various doses, which will be based on the natural doses of hesperidin present in citrus fruits or juice to extrapolate the results from rats to humans.

In conclusion, hesperidin supplementation for 8 weeks can change the proteomic profiles of the heart and kidney tissues in MS rats and has a beneficial impact on the cardiovascular system, free radical scavenging, and lipid and glucose metabolism. Therefore, the identification of proteins involved in metabolic pathways can help to understand the molecular basis of hesperidin in MS rats. However, further research is needed to confirm the results reported in the present study in humans.

5. REFERENCES

[1] Zhao, C.N., Meng, X., Li, Y., Li, S., Liu, Q., Tang, GY., Li, HB. sFruits for prevention and treatment of cardiovascular diseases. *Nutrients* 2017, *9*, 1–29.

[2] Alissa, E.M., Ferns, G.A., Dietary fruits and vegetables and cardiovascular diseases risk. *Crit. Rev. Food Sci. Nutr.* 2017, *57*, 1950–1962.

[3] World Health Organization, WHO | Top 10 causes of death. *WHO* 2018.

[4] Serino, A., Salazar, G., Protective role of polyphenols against vascular inflammation, aging and cardiovascular disease. *Nutrients* 2019, *11*, 1–23.

[5] Rienks, J., Barbaresko, J., Nöthlings, U., Association of polyphenol biomarkers with cardiovascular disease and mortality risk: A systematic review and Meta-Analysis of observational studies. *Nutrients* 2017, *9*.

[6] Cui, Z., Dewey, S., Gomes, A. V, Cardioproteomics: advancing the discovery of signaling mechanisms involved in cardiovascular diseases. *Am. J. Cardiovasc. Dis.* 2011, *1*, 274–92.

[7] Mokou, M., Lygirou, V., Vlahou, A., Mischak, H., Proteomics in cardiovascular disease: recent progress and clinical implication and implementation. *Expert Rev. Proteomics* 2017, *14*, 117–136.

[8] Yamamoto, M., Jokura, H., Hashizume, K., Ominami, H., Shibuya, Y., Suzuki, A., Hase, T., Shimotoyodome, A. Hesperidin metabolite hesperetin-7-O-glucuronide, but not hesperetin-3′-O-glucuronide, exerts hypotensive, vasodilatory, and anti-inflammatory activities. *Food Funct.* 2013, *4*, 1346.

[9] Homayouni, F., Haidari, F., Hedayati, M., Zakerkish, M., Ahmadi, K. Blood pressure lowering and anti-inflammatory effects of hesperidin in type 2 diabetes; a randomized double-blind controlled clinical trial. *Phyther. Res.* 2018, *32*, 1073–1079.

[10] Rangel-Huerta, O.D., Aguilera, C.M., Martin, M. V., Soto, M.J., Rico, MC., Vallejo, F., Tomas-Barberan, F., Perez-de-la-Cruz, AJ., Gil, A., Mesa, MD. Normal or High Polyphenol Concentration in Orange Juice Affects Antioxidant Activity, Blood Pressure, and Body Weight in Obese or Overweight Adults. *J. Nutr.* 2015, *145*, 1808–1816.

[11] Wunpathe, C., Potue, P., Maneesai, P., Bunbupha, S., Prachaney, P., Kugongviriyapan, U., Kugongviriyapan, V., Pakdeechote, P. Hesperidin Suppresses Renin-Angiotensin System Mediated NOX2 Over-Expression and Sympathoexcitation in 2K-1C Hypertensive Rats. *Am. J. Chin. Med.* 2018, *46*, 1–17.

[12] Dobiaš, L., Petrová, M., Vojtko, R., Kristová, V., Long-term Treatment with Hesperidin Improves Endothelium-dependent Vasodilation in Femoral Artery of Spontaneously Hypertensive Rats: The Involvement of NO-synthase and K_v Channels. *Phyther. Res.* 2016, *30*, 1665–1671.

[13] Jia, S., Hu, Y., Zhang, W., Zhao, X., et al., Hypoglycemic and hypolipidemic effects of neohesperidin derived from Citrus aurantium L. in diabetic KK-A^y mice. *Food Funct.* 2015, *6*, 878–886.

[14] Sun, Y.Z., Chen, J.F., Shen, L.M., Zhou, J., Chen, Y., Sun, C., Li, X., Chen, K. Anti-atherosclerotic effect of hesperidin in LDLr−/−mice and its possible mechanism. *Eur. J. Pharmacol.* 2017, *815*, 109–117.

[15] Iskender, H., Dokumacioglu, E., Sen, T.M., Ince, I., Kanbay, Y., Saral, S. The effect of hesperidin and quercetin on oxidative stress, NF-κB and SIRT1 levels in a STZ-induced experimental diabetes model. *Biomed. Pharmacother.* 2017, *90*, 500–508.

[16] Maneesai, P., Bunbupha, S., Potue, P., Berkban, T., Kugongviriyapan, U., Kukongviriyapan, V., Prachaney, P., Pakdeechote, P. Hesperidin prevents nitric oxide deficiency-induced cardiovascular remodeling in rats via suppressing TGF-β1 and MMPsprotein expression. *Nutrients* 2018, *10*, 1–15.

[17] Lerma-García, M.J., D'Amato, A., Simó-Alfonso, E.F., Righetti, P.G., Fasoli, E. Orange proteomic fingerprinting: From fruit to commercial juices. *Food Chem.* 2016, *196*, 739–749.

[18] Wang, J. hui, Liu, J. jun, Chen, K. ling, Li, H. wen, Guan, B., He, L. Comparative transcriptome and proteome profiling of two Citrus sinensis cultivars during fruit development and ripening. *BMC Genomics* 2017, *18*, 1–13.

[19] Chaves, D.F.S., Carvalho, P.C., Brasili, E., Rogero, M.M., Hassimotto, NMA., Diedrich, JK., Moresco, JJ., Yates, JR., Lajolo, FM. Proteomic Analysis of Peripheral Blood Mononuclear Cells after a High-Fat, High-Carbohydrate Meal with Orange Juice. *J. Proteome Res.* 2017, *16*, 4086–4092.

[20] Yumnam, S., Saralamma, V.V.G., Raha, S., Lee, H.J., Suplee, W., Kim, EH., Lee, SJ., Heo, JD., Kim GS. Proteomic profiling of human HepG2 cells treated with hesperidin using antibody array. *Mol. Med. Rep.* 2017, *16*, 5386–5392.

[21] Guirro, M., Costa, A., Gual-Grau, A., Mayneris-Perxachs, J., Torrell, H., Herrero, P., Canela, N., Arola, L. Multi-omics approach to elucidate the gut microbiota activity: Metaproteomics and metagenomics connection. *Electrophoresis* 2018, *39*, 1692–1701.

[22] Mosqueda-Solís, A., Sánchez, J., Reynés, B., Palou, M., Palou, A., Picó, C. Hesperidin and capsaicin, but not the combination, prevent hepatic steatosis and other metabolic syndrome-related alterations in western diet-fed rats. *Sci. Rep.* 2018, *8*, 1–14.

[23] Reagan-Shaw, S., Nihal, M., Ahmad, N., Dose translation from animal to human studies revisited. *FASEB J.* 2008, *22*, 659–661.

[24] Guirro, M., Gual-grau, A., Gibert-ramos, A., Alcaide-hidalgo, J.M., Canela, N., Arola, L.,

391 Mayneris-Perxachs, J. Metabolomics Elucidates Dose-Dependent Molecular Beneficial E ff ects
392 of Hesperidin Supplementation in Rats Fed an Obesogenic Diet. n.d., 1–19.
393 [25] Alberti, K.G.M.M., Eckel, R.H., Grundy, S.M., Zimmet, P.Z., Cleeman, JI., Donato, KA.,
394 Fruchart, JC., James, WPT., Loria, CM., Smith, SC. Harmonizing the metabolic syndrome: A
395 joint interim statement of the international diabetes federation task force on epidemiology and
396 prevention; National heart, lung, and blood institute; American heart association; World heart
397 federation; International . *Circulation* 2009, *120*, 1640–1645.
398 [26] Nøhr, M.K., Kroager, T.P., Sanggaard, K.W., Knudsen, A.D., Stensballe, A., Enghild, J., Olholm,
399 J., Richelsen, B., Pedersen SB. SILAC-MS based characterization of LPS and resveratrol induced
400 changes in adipocyte proteomics - Resveratrol as ameliorating factor on LPS induced changes.
401 *PLoS One* 2016, *11*, 1–16.
402 [27] Catalán, Ú., Rubió, L., López de Las Hazas, M.C., Herrero, P., Nadal, P., Canela, N., Pedret, A.,
403 Motilva, MJ., Solà, R. Hydroxytyrosol and its complex forms (secoiridoids) modulate aorta and
404 heart proteome in healthy rats: Potential cardio-protective effects. *Mol. Nutr. Food Res.* 2016, *60*,
405 2114–2129.
406 [28] Pedret, A., Catalán, Ú., Fernández-Castillejo, S., Farràs, M., Valls, RM., Rubió, L., Canela, N.,
407 Aragonés, G., Romeu, M., Castañer, O., Torre, R., Covas, MI., Fitó, M., Motilva, MJ, Solà, R.
408 Impact of virgin olive oil and phenol-enriched virgin olive oils on the HDL proteome in
409 hypercholesterolemic subjects: A double blind, randomized, controlled, cross-over clinical trial
410 (VOHF study). *PLoS One* 2015, *10*, 1–19.
411 [29] Pritchard, T.J., Parvatiyar, M., Bullard, D.P., Lynch, R.M., Lorenz, JN., Paul, RJ. Transgenic mice
412 expressing Na + -K + -ATPase in smooth muscle decreases blood pressure . *Am. J. Physiol. Circ.*
413 *Physiol.* 2007, *293*, H1172–H1182.
414 [30] Osanai, T., Sasaki, S., Kamada, T., Fujiwara, N., et al., Circulating coupling factor 6 in human
415 hypertension: Role of reactive oxygen species. *J. Hypertens.* 2003.
416 [31] He, T., Guan, A., Shi, Y., Ge, Z., Dai, H. Hochregulation von „mitochondrial coupling factor 6“
417 bei hypertonieinduzierter kardialer Hypertrophie. *Herz* 2015, *40*, 783–787.
418 [32] Pinkaew, D., Fujise, K., Fortilin: A Potential Target for the Prevention and Treatment of Human

Diseases. *Adv. Clin. Chem.* 2017, *82*, 265–300.

[33] P.U., G., H.K., G., M.J., S., J.L., J., et al., Insulin-Like Growth Factor-Binding Protein-7 as a Biomarker of Diastolic Dysfunction and Functional Capacity in Heart Failure With Preserved Ejection Fraction: Results From the RELAX Trial. *JACC Hear. Fail.* 2016.

[34] Brocker, C., Cantore, M., Failli, P., Vasiliou, V., Aldehyde dehydrogenase 7A1 (ALDH7A1) attenuates reactive aldehyde and oxidative stress induced cytotoxicity, in: *Chemico-Biological Interactions*, 2011.

[35] Negre-Salvayre, A., Auge, N., Ayala, V., Basaga, H., Boada, J., Brenke, R., Chapple, S., Cohen, G., Feher, J., Grune, T., Lengyel, G., Mann, GE., Pamplona, R., Poli, G., Portero-otin, M., Riahi, Y., Salvayre, R., Sasson, S., Serrano, J., Shamni, O., Siems, W., Siow, RCM., Wiswedel, I., Zarkovic, K., Zarkovic, N. Pathological aspects of lipid peroxidation. *Free Radic. Res.* 2010, *44*, 1125–1171.

[36] Nakanishi, T., Markwald, R.R., Baldwin, H.S., Keller, B.B., et al., Etiology and morphogenesis of congenital heart disease: From gene function and cellular interaction to morphology. *Etiol. Morphog. Congenit. Hear. Dis. From Gene Funct. Cell. Interact. to Morphol.* 2016, 1–383.

[37] Chen, A., Chen, Z., Xia, Y., Lu, D., Jia, J., Hu, K., Sun, A., Zou, Y, Qian, J., Ge, J. Proteomics analysis of myocardial tissues in a mouse model of coronary microembolization. *Front. Physiol.* 2018, *9*, 1–10.

[38] Toomer, K., Sauls, K., Fulmer, D., Guo, L., Moore, K., Glover, J., Stairley, R., Bischoff, J., Levine, RA., Norris, RA. Filamin-A as a Balance between Erk/Smad Activities During Cardiac Valve Development. *Anat. Rec.* 2019, *302*, 117–124.

[39] Jain, M., Mann, T.D., Stulić, M., Rao, S.P., Kirsch, Andrijana., Pullirsch, D., Strobl, S., Rath, C., Reissing, L., Moreth, K., Klein-Rodewald, T., Bekeredjian, R., Gailus-Durner, V., Fuchs, H., Angelis, MH., Pablik, E., Cimatti, L., Martin, D., Zinnanti, J., Graier, WF., Sibilia, M., Frank, S., Levanon, EY., Jantsch, MF. RNA editing of Filamin A pre-mRNA regulates vascular contraction and diastolic blood pressure. *EMBO J.* 2018, *37*, e94813.

[40] Huber, T.B., Hartleben, B., Kim, J., Schmidts, M., Schermer, B., Keil, A., Egger, L., Lecha, RL., Borner, C., Pavenstadt, H., Shaw, AS., Walz, G., Benzing, T. Nephrin and CD2AP associate with

447 phosphoinositide 3-OH kinase and stimulate AKT-dependent signaling. *Mol. Cell. Biol.* 2003, *23*,
448 4917–28.
449 [41] Hyvönen, M.E., Ihalmo, P., Sandholm, N., Stavarachi, M., Farsblom, C., McKnight, AJ., Lajer,
450 M., Maestroni, A., Lewis, G., Tanow, L., Maestroni, S., Zerbini, G., Parving, HH., Maxwell, AP.,
451 Groop, PH., Lehtonnen, S. CD2AP is associated with end-stage renal disease in patients with type
452 1 diabetes. *Acta Diabetol.* 2013, *50*, 887–897.
453 [42] Ramirez, C.E., Shuey, M.M., Milne, G.L., Gilbert, K., Hui, N., Yu, C., Luther, JM., Brown, NJ.
454 Arg287Gln variant of EPHX2 and epoxyeicosatrienoic acids are associated with insulin sensitivity
455 in humans. *Prostaglandins Other Lipid Mediat.* 2014.
456 [43] Kobayashi, K., Monkawa, T., Hayashi, M., Saruta, T., Expression of the Na+/H+ exchanger
457 regulatory protein family in genetically hypertensive rats. *J. Hypertens.* 2004, *22*, 1723–1730.
458 [44] Verhague, M.A., Cheng, D., Weinberg, R.B., Shelness, G.S., Apolipoprotein A-IV expression in
459 mouse liver enhances triglyceride secretion and reduces hepatic lipid content by promoting very
460 low density lipoprotein particle expansion. *Arterioscler. Thromb. Vasc. Biol.* 2013, *33*, 2501–
461 2508.
462 [45] Kohan, A.B., Wang, F., Li, X., Vandersall, A.E., Huesman, S., Xu, M., Yang, Q., Lou, D., Tso, P.
463 Is apolipoprotein A-IV rate limiting in the intestinal transport and absorption of triglyceride? *Am.*
464 *J. Physiol. Liver Physiol.* 2013, *304*, G1128–G1135.
465 [46] Palmieri, F., The mitochondrial transporter family SLC25: Identification, properties and
466 physiopathology. *Mol. Aspects Med.* 2013, *34*, 465–484.
467 [47] Gao, F., Liu, Q., Li, G., Dong, F., Qiu, M., Lv, X., Zhang, S., Guo, Z. Identification of ubiquinol
468 cytochrome c reductase hinge (UQCRH) as a potential diagnostic biomarker for lung
469 adenocarcinoma. *Open Biol.* 2016, *6*.
470 [48] Park, E.R., Kim, S.B., Lee, J.S., Kim, Y.H., Lee, DH., Cho, EH., Park, SH., Han, CJ., Kim, BY.,
471 Choi, DW., Yoo, YD., Yu, A., Lee, JW., Jang, JJ., Park YN., Suh, KS., Lee, KH. The
472 mitochondrial hinge protein, UQCRH, is a novel prognostic factor for hepatocellular carcinoma.
473 *Cancer Med.* 2017, *6*, 749–760.
474 [49] Wei, Q., Zhou, W., Wang, W., Gao, B., Wang, L., Cao, J., Liu, ZP. Tumor-suppressive functions

of leucine zipper transcription factor-like 1. *Cancer Res.* 2010.

[50] Ferreira de Oliveira, J.M.P., Santos, C., Fernandes, E., Therapeutic potential of hesperidin and its aglycone hesperetin: Cell cycle regulation and apoptosis induction in cancer models. *Phytomedicine* 2019, 152887.

[51] Zhao, J., Li, Y., Gao, J., De, Y., Hesperidin inhibits ovarian cancer cell viability through endoplasmic reticulum stress signaling pathways. *Oncol. Lett.* 2017, *14*, 5569–5574.

ACKNOWLEDGMENTS

Funding

This research was cofunded by the 7th Framework Program of the European Union and the Agency for Business Competitiveness of the Government of Catalonia (ACCIÓ) under the TECNOspring program awarded to JM-P (TECSPR14-2-0001). AP has a Torres Quevedo contract (Subprograma Estatal de Incorporación, Plan Estatal de Investigación Científica y Técnica y de Innovación). UC has a Pla Estratègic de Recerca i Innovació en Salut postdoctoral grant (SLT0021/16/00239); Catalunya, Spain).

Author contributions

MG, AG-G, AGR and JM-P performed the experimental study in rats. NC and EF-R performed the proteomic analysis. LP-P analyzed the proteomic results under the supervision of UC and LP-P wrote the manuscript. UC, NC, JM-P, RMV, LLA, RS and AP provided feedback on the manuscript.

Conflict of interest

The authors have no conflicts of interest to declare.

Table 1. Thirty-five proteins differentially expressed in heart tissue after hesperidin treatment in CAFH compared to CAFV rats.

UniProt code	Gene symbol	Protein description	MW (kDa)	Univariate analysis		Multivariate analysis
				FC	*p*-value[a]	VIP[b]
M0RDK9	ACAD8	Acyl-CoA dehydrogenase family, member 8	45.10	1.4409	0.0044	1.8469
F1LN92	AFG3L2	AFG3-like matrix AAA peptidase subunit 2	89.30	1.3967	0.0060	1.7448
Q64057	ALDH7A1	Alpha-aminoadipic semialdehyde dehydrogenase	58.70	1.2888	0.0004	1.6283
P02651	APO A4	Apolipoprotein A-IV	44.40	-1.5095	0.0093	1.9047
P19939	APO C1	Apolipoprotein C-I	9.90	1.7180	0.0033	2.2661
G3V8D4	APO C2	Apolipoprotein C-II	10.70	-1.8310	0.0006	2.4926
P06685	ATP1A1	Sodium/potassium-transporting ATPase subunit alpha-1	113.00	1.3297	0.0020	1.6668
G3V7Y3	ATP5F1D	ATP synthase subunit delta, mitochondrial	17.60	-1.3813	0.0047	1.7317
D4A305	CCDC58	Coiled-coil domain containing 58, isoform CRA_c	16.70	1.7327	0.0065	2.2324
Q8CFN2	CDC42	Cell division control protein 42 homolog	21.20	1.2746	0.0025	1.5289
Q5XIM5	CDV3	Protein CDV3 homolog	24.30	-1.6055	0.0040	2.1074
M0RC65	CFL2	Cofilin 2	18.70	-1.3380	0.0054	1.635
F1M779	CLTC	Clathrin heavy chain	191.40	1.2960	0.0024	1.5829
Q5BJQ0	COQ8A	Atypical kinase COQ8A, mitochondrial	72.20	-1.2667	0.0012	1.5373
P11240	COX5A	Cytochrome c oxidase subunit 5A, mitochondrial	16.10	-1.5030	0.0056	1.9324
P60841	ENSA	Alpha-endosulfine	NA	-1.2770	0.0034	1.5225
C0JPT7	FLNA	Filamin A	280.30	1.5440	0.0007	2.1071
D3ZT90	GCDH	Glutaryl-CoA dehydrogenase	49.70	1.2996	0.0050	1.5552
Q5I0P2	GCSH	Glycine cleavage system H protein, mitochondrial	18.50	-1.5136	0.0097	1.9064
D4ADD7	GLRX5	Glutaredoxin 5	16.40	-1.2978	0.0019	1.5977
D4A4L5	ISCA2	Iron-sulfur cluster assembly 2	16.70	-1.3870	0.0098	1.6936
G3V6P7	MYH9	Myosin, heavy polypeptide 9, nonmuscle	226.30	1.8328	0.0019	2.4356

A0A0G2KAQ5	MYOZ2	Myozenin 2	29.80	-1.4006	0.0084	1.7298
Q5XI78	OGDH	2-oxoglutarate dehydrogenase, mitochondrial	116.20	1.3004	0.0043	1.5656
P04916	RBP4	Retinol-binding protein 4	23.20	-1.3708	0.0037	1.7246
G3V8R0	RGD1311703	Similar to sid2057p	19.90	-1.5060	0.0053	1.9425
F1LSW7	RPL14	60S ribosomal protein L14	23.30	1.3440	0.0021	1.6981
Q6IRH6	SLC25A3	Phosphate carrier protein, mitochondrial	39.60	1.3677	0.0098	1.5331
P97849	SLC27A1	Long-chain fatty acid transport protein 1	71.20	1.2016	0.0037	1.5028
P07632	SOD1	Superoxide dismutase[Cu-Zn]	15.90	-1.39760	0.0040	1.7717
P62078	TIMM8B	Mitochondrial import inner membrane translocase subunit Tim8 B	9.30	-1.5168	0.0073	1.9335
P62074	TIMM10	Mitochondrial import inner membrane translocase subunit Tim10	10.30	-1.2840	0.0043	1.5285
Q5XIK2	TMX2	Thioredoxin-related transmembrane protein 2	33.80	1.4949	0.0031	1.9565
B0K010	TXNDC17	Thioredoxin domain-containing 17	14.10	-1.3020	0.0052	1.5612
Q5M9I5	UQCRH	Cytochrome b-c1 complex subunit 6 mitochondrial	10.40	-1.4631	0.0037	1.8937

CAFH, metabolic syndrome rats with hesperidin supplementation; CAFV, metabolic syndrome rats without hesperidin supplementation; MW, molecular weight; FC, fold change; NA, not available.
[a]Results from Wilcoxon tests and t-test. A p-value<0.01 was considered statistically significant.
[b]VIP score was from PLS-DA.

Table 2. Fifty-three proteins differentially expressed in kidney tissue after hesperidin treatment in CAFH compared to CAFV rats.

UniProt code	Gene symbol	Protein description	MW (kDa)	Univariate analysis		Multivariate analysis
				FC	*p*-value[a]	VIP[b]
Q80W57	ABCG2	ATP-binding cassette subfamily G member 2	72.90	1.2570	0.0031	1.6966
Q6P2A5	AK3	GTP:AMP phosphotransferase AK3, mitochondrial	25.50	-1.2561	0.0094	1.7174
Q9WUC4	ATOX1	Copper transport protein ATOX1	7.30	-1.2888	0.0021	1.8082
Q03344	ATP5IF1	ATPase inhibitor, mitochondrial	12.20	-1.3651	0.0005	2.0549
P21571	ATP5PF	ATP synthase-coupling factor 6, mitochondrial	12.50	-1.6119	0.0028	2.4703
B2GUV5	ATP6V1G1	V-type proton ATPase subunit G	13.70	-1.4949	0.0014	2.2956
Q5I0M1	APO H	Apolipoprotein H	38.40	-1.5042	0.0008	2.3359
F1LRS8	CD2AP	CD2-associated protein	70.40	-1.2746	0.0088	1.6887
D3ZD09	COX6B1	Cytochrome c oxidase subunit	10.10	-1.4006	0.009	1.9883
P32198	CPT1A	Carnitine O-palmitoyltransferase 1, liver isoform	88.10	1.4794	0.0043	2.1983
P97829	CD47	Leukocyte surface antigen CD47	33.00	1.2059	0.0038	1.5247
Q8CFN2	CDC42	Cell division control protein 42 homolog	21.20	1.2033	0.0033	1.5261
D3ZUX5	CHCHD3	MICOS complex subunit	26.40	-1.3168	0.0022	1.8771
A0A0H2UHL6	CTSH	Pro-cathepsin H	32.90	-1.6982	0.0038	2.5675
P07154	CTSL	Cathepsin L1	37.60	1.5305	0.0035	2.3057
Q68FR9	EEF1D	Elongation factor 1-delta	31.30	-1.2527	0.0035	1.6775
A3E0T0	EPB41L3	Erythrocyte membrane protein band 4.1-like 3	96.90	-1.5757	0.0065	2.3375
P80299	EPHX2	Bifunctional epoxide hydrolase 2	62.30	4.2663	0.0087	4.1318
C0JPT7	FLNA	Filamin A	280.30	1.2067	0.005	1.5157
P19468	GCLC	Glutamate-cysteine ligase catalytic subunit	72.60	1.3370	0.0008	1.9709
D3ZK97	H3F3C	Histone H3	15.30	1.2772	0.0097	1.691
F1M9B2	IGFBP7	Insulin-like growth factor binding protein 7, isoform CRA_b	28.90	-1.6947	0.0024	2.593
D4A4L5	ISCA2	Iron-sulfur cluster assembly 2	16.70	-1.3918	0.0055	2.0032
B2RZ79	ISCU	Iron-sulfur cluster assembly enzyme	18.00	-1.3077	0.0013	1.8767

D3ZCZ9	LOC100912599	NADH dehydrogenase [ubiquinone] iron-sulfur protein 6, mitochondrial	13.00	-1.2978	0.0037	1.8041
Q562C6	LZTFL1	Leucine zipper transcription factor-like protein 1	34.60	-1.5810	0.0012	2.4546
D3Z900	MARC2	Mitochondrial amidoxime reducing component 2	38.20	1.2501	0.0009	1.7259
A0A0H2UHX5	MME	Neprilysin	78.60	1.2870	0.0062	1.745
Q63357	MYO1D	Unconventional myosin-Id	116.00	1.4044	0.0072	2.0134
G3V8R1	NUCB2	Nucleobindin 2. isoform CRA_b	50.10	-1.3538	0.0042	1.9359
Q5XI78	OGDH	2-oxoglutarate dehydrogenase, mitochondrial	116.20	1.2142	0.0003	1.6381
P51583	PAICS	Multifunctional protein ADE2	47.10	1.4550	0.0078	2.1091
D3ZD40	PAPLN	Papilin. proteoglycan-like sulfated glycoprotein	138.50	-1.4040	0.0046	2.0433
B0BN18	PFDN2	Prefoldin subunit 2	16.60	-1.2527	0.0065	1.6467
P85973	PNP	Purine nucleoside phosphorylase	32.30	1.3718	0.0005	2.0718
P10960	PSAP	Prosaposin	61.10	-1.4641	0.0057	2.151
P63245	RACK1	Receptor of activated protein C kinase 1	35.10	1.2130	0.0005	1.6195
Q6TXG7	SHMT1	Serine hydroxymethyltransferase	75.30	1.2142	0.0042	1.5493
F1LZW6	SLC25A13	Solute carrier family 25 member 13	54.10	1.2303	0.0023	1.6277
G3V741	SLC25A3	Phosphate carrier protein. mitochondrial	39.50	1.2050	0.0057	1.5022
Q9JJ19	SLC9A3R1	Na(+)/H(+) exchange regulatory cofactor NHE-RF1	38.80	-1.2588	0.0093	1.6398
G3V6D9	SLC9A3R2	Na(+)/H(+) exchange regulatory cofactor NHE-RF	37.30	-1.2467	0.0061	1.6295
P07632	SOD1	Superoxide dismutase[Cu-Zn]	15.90	-1.5801	0.0036	2.3891
A0A0G2K9X1	SPP2	Secreted phosphoprotein 24	14.90	-1.5094	0.004	2.2601
O70257	STX7	Syntaxin-7	28.80	-1.3122	0.0085	1.7901
P62078	TIMM8B	Mitochondrial import inner membrane translocase subunit Tim8 B	9.30	-1.5241	0.0058	2.2588
Q63610	TPM3	Tropomyosin alpha-3 chain	29.00	-1.4241	0.0036	2.1009
P09495	TPM4	Tropomyosin alpha-4 chain	28.50	-1.3918	0.0056	2.0044
P63029	TPT1	Translationally controlled tumor protein	19.40	-1.4459	0.0027	2.163
P97615	TXN2	Thioredoxin. mitochondrial	18.20	-1.3698	0.0075	1.9353

Q5M9I5	UQCRH	Cytochrome b-c1 complex subunit 6, mitochondrial	10.40	-1.4015	0.0027	2.0703
Q9Z269	VAPB	Vesicle-associated membrane protein-associated protein B	26.90	-1.3168	0.0097	1.7924
A0A0G2JSR0	VDAC3	Voltage-dependent anion-selective channel protein 3	30.80	1.2226	0.0006	1.6488

CAFH, metabolic syndrome rats with hesperidin supplementation; CAFV, metabolic syndrome rats without hesperidin supplementation; MW, molecular weight; FC, fold change.
[a]Results from Wilcoxon tests and t-tests. A p-value<0.01 was considered statistically significant.
[b]VIP score was from PLS-DA.

Table 3. Top diseases and functions determined by heart and kidney tissue proteomic analyses in CAFH compared to CAFV rats.

Categories		Heart tissue proteins	Kidney tissue proteins
Cardiovascular system	Development of neointima	-	↓TPT1
	Blood pressure	-	↓ATP5PF, ↑EPHX2, ↓SOD1
	Density of microvessel	-	↑EPHX2
	Angiogenesis	-	↑Cdc42, ↑EPHX2, ↓TPT1
	Binding of endothelial cells	-	↑CD47
	Sprouting angiogenesis	↑Cdc42	↑CDC42
	Heart rate	↑ATP1A1, ↓SOD1	-
	Ischemic acute renal failure	↑ATP1A1	-
Free radical scavenging	Metabolism, removal and quantity of superoxide	↓SOD1	↓SOD1
	Biosynthesis of hydrogen peroxide	↓SOD1	-
Lipid metabolism	Fatty acid metabolism	↑OGDH, ↓APOA4, ↑APOC1, ↑GCDH, ↓RBP4, ↑SLC27A1	↑OGDH, ↓APOH, ↓ATP5PF, ↑CPT1A, ↑EPHX2, ↓IGFBP7
	Transport of lipid	↓APOA4, ↑APOC1, ↓RBP4, ↑SLC27A1	-
	Metabolism of lipoprotein	↑APOC1	-
	Synthesis of epoprostenol	-	↓ATP5PF, ↓IGFBP7
	Synthesis of prostaglandin	-	↓ATP5PF, ↑EPHX2, ↓IGFBP7
	Binding of eicosapentenoic acid and malonyl-coenzyme A	-	↑CPT1A
	Beta-oxidation of oleic acid	-	↑CPT1A
	Transport of triacylglycerol	-	↓APOH
	Quantity of long-chain acyl-coenzyme A	-	↑CPT1A
	Metabolism of succinyl-coenzyme A	↑OGDH	↑OGDH
	Accumulation of triacylglycerol	-	↑CPT1A
	Oxidation of fatty acid	↑GCDH, ↑SLC27A1	↑CPT1A, ↓NUCB2
	Metabolism of long chain fatty acids	-	↑CPT1A

	Esterification, transport and oxidation of palmitic acid	↑SLC27A1	↑CPT1A
	Synthesis and metabolism of acyl-coenzyme A	↑GCDH, ↑OGDH	-
	Transport of retinol	↓RBP4	-
Glucose metabolism	Insulin sensitivity index	-	↓NUCB2
	Secretion of glucagon	-	↓NUCB2
Renal and urological disease	Nephrosis	↑CLTC	-
	Apoptosis of kidney cells	↑ATP1A1, ↑CDC42	-

CAFH, metabolic syndrome rats with hesperidin supplementation; CAFV, metabolic syndrome rats without hesperidin supplementation; -, no protein identified; ↑, protein upregulated; ↓, protein downregulated.

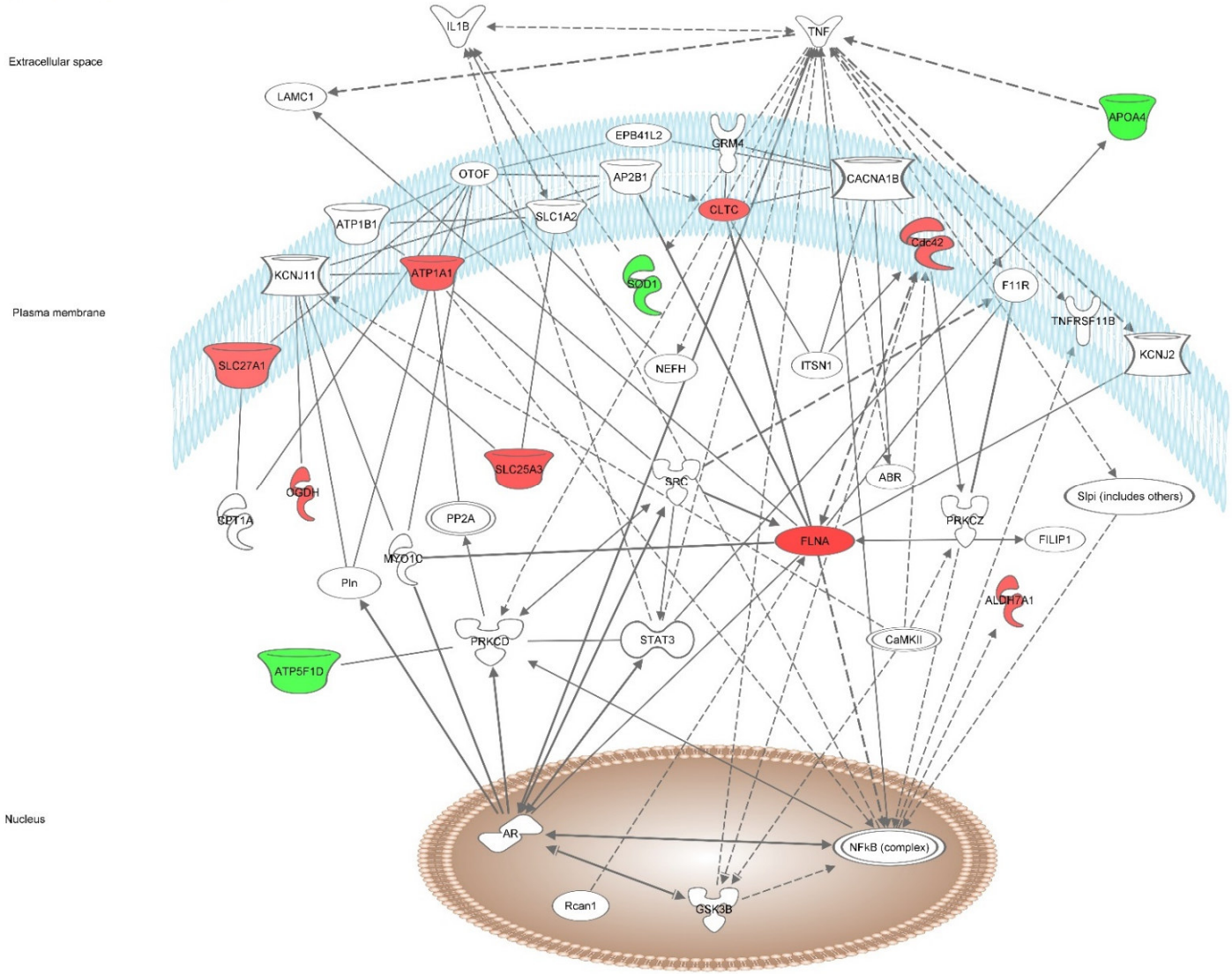

Figure 1. Graphical representation of the top networks of the heart tissue proteome after hesperidin supplementation. Interaction between the differentially expressed proteins and other important proteins. Down- and upregulated proteins are symbolized in red and green, respectively. ABR, active breakpoint cluster region-related protein; ALDH7A1, aldehyde dehydrogenase 7 family member 1; AP2B1, AP-2 complex subunit beta; APOA4, apolipoprotein A4; ATP1A1, ATPase Na+/K+ transporting subunit alpha 1; ATP1B1, sodium/potassium-transporting ATPase subunit beta-1; ATP5F1D, ATP synthase F1 subunit delta; CACNA1B, voltage-dependent N-type calcium channel subunit alpha-1B; CAMKII, calcium/calmodulin-dependent protein kinase type II alpha chain; CDC42, cell division cycle 42; CLTC, clathrin heavy chain; CPT1A, carnitine palmitoyltransferase 1A; EPB41L2, erythrocyte membrane protein band 4.1-like 2; F11R, junctional adhesion molecule A; FILIP1, filamin-A-interacting protein 1; GRM4, metabotropic glutamate receptor 4; IL1B, interleukin-1 beta; ITSN1, intersection-1; FLNA, filamin A; KCNJ11, ATP-sensitive inward rectifier potassium channel 11; KCNJ2, inward rectifier potassium channel 2; LAMC1, laminin subunit gamma 1; MYO1C, unconventional myosin-Ic; NEFH, neurofilament heavy

polypeptide; NFKB, nuclear factor NF-kappa-B p105 subunit; OGDH, oxoglutarate dehydrogenase; OTOF, otoferlin; PIN, peptidyl-propyl cis-trans isomerase NIMA-interacting 1; PP2A, serine/threonine-protein phosphatase 2A 55 kDa regulatory subunit B beta isoform; PRKCD, protein kinase C delta type; SRC, proto-oncogene tyrosine-protein kinase Src; PRKCZ, protein kinase C zeta type; RCAN1, calcipressin-1; GSK3B, glycogen synthase kinase-3 beta; SIPI, secretory leukocyte protease inhibitor; AR, androgen receptor; SLC1A2, excitatory amino acid transporter 2; SLC25A3, solute carrier family 25 member 3; SLC27A1, long-chain fatty acid transport protein 1; SOD1, superoxide dismutase 1; STAT3, signal transducer and activator of transcription 3; TNF, tumor necrosis factor; TNFRSF11B, tumor necrosis factor receptor superfamily member 11B.

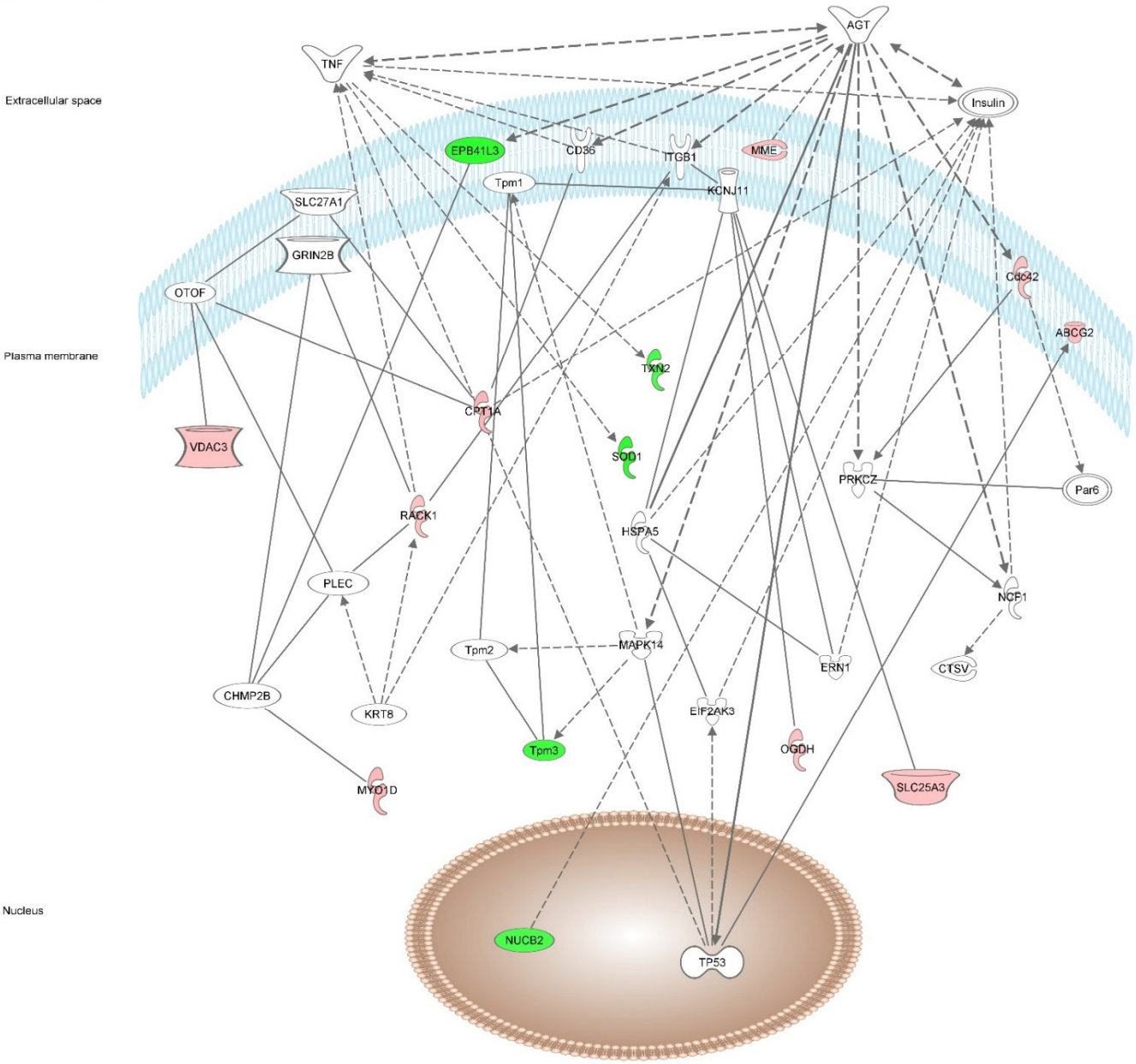

Figure 2. Graphical representation of the top networks of the kidney tissue proteome after hesperidin supplementation. Interaction between the differentially expressed proteins and other important proteins. Down- and upregulated proteins are symbolized in red and green, respectively. ABCG2, ATP binding cassette subfamily G member 2; AGT, angiotensinogen; CD36, CD36 molecule (trombospondin receptor); CDC42, cell division cycle 42; CHMP2B, charged multivesicular body protein 2B; CPT1A, carnitine palmitoyltransferase 1A; CTSV, cathepsin V; EIF2AK3, eukaryotic translation initiation factor 2-alpha kinase 3; EPB41IL3, erythrocyte membrane protein band 4.1-like 3; ERN1, endoplasmic reticulum to nucleus-signaling 1; GRIN2B, glutamate receptor ionotropic NMDA 2B; HSPA5, endoplasmic reticulum chaperone BiP; ITGB1, integrin beta-1; KCNJ11, ATP-sensitive inward rectifier potassium channel 11; KRT8, keratin type II cytoskeletal 8; MAPK14, mitogen-activated protein kinase 14; MME, neprilysin;

MYO1D, unconventional myosin-Id; NCF1, neutrophil cytosolic factor 1; NUCB2, nucleobindin 2; OGDH, oxoglutarate dehydrogenase; OTOF, otoferlin; PAR6, partitioning defective 6 homolog alpha; PLEC, plectin; PRKCZ, protein kinase C zeta type; RACK1, receptor of activated protein C kinase 1; SLC25A3, solute carrier family 25 member 3; SLC27A1, solute carrier family 27 member 1; SOD1, superoxide dismutase 1; TNF, tumor necrosis factor; TP53, cellular tumor antigen o53; TPM1, tropomyosin alpha-1 chain; TPM2, tropomyosin beta chain; TPM3, tropomyosin alpha-3 chain; TXN2, thioredoxin mitochondrial; VDAC3, voltage-dependent anion-selective channel protein 3.